Fatigue & Fracture of Engineering Materials & Structures 1998; **21**: 1317–1325

EFFECT OF GRAIN SIZE ON COLLECTIVE DAMAGE OF SHORT CRACKS AND FATIGUE LIFE ESTIMATION FOR A STAINLESS STEEL

Y. HONG, Y. QIAO, N. LIU[1] and X. ZHENG[1]

Laboratory for Non-linear Mechanics of Continuous Media (LNM), Institute of Mechanics, Chinese Academy of Sciences, Beijing 100080, China

[1]Beijing Institute of Technology, Beijing 100081, China

Abstract—In the short crack regime of the fatigue process, grain boundaries in steels are barriers against crack growth. In this paper, we use: (1) a method involving crack density; and (2) a method of dimensional analysis, to evaluate the effects of grain size and grain-boundary resistance on short crack behaviour and fatigue life. The results show that the fatigue life increases with a decrease in grain size and an enlargement in the obstacle effect of a grain boundary. An experimental investigation is consequently performed and four groups of stainless steel specimens are used with different grain sizes. The experimental measurements show the dependence of fatigue properties on grain size, which are in good agreement with the theoretical results.

Keywords—Short fatigue cracks; Fatigue life; Grain size effect; Stainless steel; Crack density; Dimensional analysis.

NOMENCLATURE

$A(c)$ = non-dimensional crack growth rate
A^* = characteristic crack growth rate
A_d = crack growth rate at $c = 1$
c = non-dimensional crack length
c_1 = the maximum crack length in the long-crack regime
c_{cr} = critical crack length characterizing the termination of the short-crack regime
d = non-dimensional grain diameter
d_0 = average grain diameter
$\bar{d}$ = normalized grain diameter ($= d/A_d$)
D = damage variable
D_0 = total number of cracks or zero-th order of the damage moment
D_1 = first order of the damage moment
G = cohesive energy of material
M = parameter related to elastic modulus and Poisson's ratio of the material
$n(c, t)$ = crack density
n^* = characteristic crack density
$n_N(c)$ = crack nucleation rate
n_N^* = characteristic crack nucleation rate
N_f = number of loading cycles to fracture
N_g = non-dimensional coefficient = $(n_N^* \cdot d/n^* \cdot A^*)$
P = parameter with respect to energy dispersion
Q = energy release rate of the damage system
r = linear correlation coefficient
t = time
t_{cr} = critical time characterizing the termination of the short-crack regime
γ = non-dimensional factor
σ = effective stress
σ_0 = nominal stress
σ_* = threshold stress for fatigue crack growth
σ_{max} = maximum stress in cyclic loading

INTRODUCTION

It is known that during the primary stage of the fatigue process in most metallic materials, fatigue damage is dominated by the behaviour of short cracks where the length of such cracks is

© 1998 Blackwell Science Ltd

comparable with a microstructural dimension, e.g. the grain size of the material. The importance of research on short fatigue cracks is due to two aspects. First, the behaviour of short cracks cannot be interpreted by conventional theories; and secondly, the period of short-crack damage may be 80% or more of the total fatigue life.

One distinct phenomenon of short crack growth has been reported, i.e. the deceleration and acceleration patterns, which has been attributed to the interaction of crack-tip plastic zone with microstructural barriers to plastic flow [1–4]. The published results of observations and the discussion of short crack behaviour are in the majority based on the monitoring of a few isolated short cracks.

However, the fatigue damage process involving short fatigue cracks in metallic materials may present collective evolution characteristics [5–10], i.e. that the damage progression may result from the initiation and growth of a large number of dispersed short cracks. One of the essential characteristics of collective damage is that the number of short cracks increases with increasing number of fatigue cycles. Since the length of short cracks is comparable to grain size, the dimension of grain diameter and the extent of the grain-boundary obstacle effect against short crack growth considerably affect the process of the collective evolution of short cracks. Such effects have been investigated to some extent in the literature, e.g. [2,5,11–14], but there is still a lack of theoretical models and systematic experiments concerning the effects of grain size and grain boundary barriers on short crack behaviour.

To deal with these two aspects of the problem, we use a new method that considers the equilibrium of crack density (ECD), in which the crack density is the number of cracks within a unit area and unit length. The concept of the model is that the total number of short cracks of a certain given length and at a given time contains the cracks that are produced by crack nucleation and growth. Consequently, we also use the method of dimensional analysis to study the evolution of fatigue damage. Both the methods mentioned above give similar analytical relationships between fatigue life and grain size. An experimental investigation was then performed, in which the test material was a stainless steel for which four groups of specimens were made having different grain sizes. The experimental results exhibit a dependence on the fatigue threshold stress and the fatigue life on grain size, which is in good agreement with the theoretical analyses.

GRAIN SIZE EFFECT USING ECD MODEL

The equilibrium equation for the crack density in non-dimensional form [14] is

$$\frac{\partial}{\partial t} n(c, t) + \frac{\partial}{\partial c} [A(c) \cdot n(c, t)] = N_g \cdot n_N(c) \tag{1}$$

This equation describes the equilibrium of crack density in the corresponding phase space. The second term on the left side of Eq. (1) represents the flow of crack density, which is attributed to crack growth, while the term on the right side represents the influence made by crack nucleation. Let $n(c, 0) = 0$ and the initial crack length before growth is zero, then the theoretical solution of Eq. (1) is [15]:

$$n(c, t) = \frac{1}{A(c)} \int_{\eta(c,t)}^{c} N_g \cdot n_N(c') \, dc' \tag{2}$$

where $\eta(c, t)$ means that a crack with length η at $t = 0$, will grow to a length c at time t under the growth rate of $A(c)$.

Taking into account the deceleration–acceleration growth of short cracks, we construct the

 © 1998 Blackwell Science Ltd

expression for $A(c)$:

$$A(c) = \begin{cases} 1-(1-A_d)c & (c \leqslant 1) \\ \bar{d} \cdot c & (c > 1) \end{cases} \tag{3}$$

where the normalized grain size $\bar{d}$ is the ratio of the non-dimensional average grain size d to A_d, the latter being the non-dimensional crack growth rate at $c = 1$. Also, according to experimental observations [7,16], we propose the formula for crack-nucleation rate:

$$n_N(c) = \begin{cases} 1 - \dfrac{c}{2} & (c \leqslant 2) \\ 0 & (c > 2) \end{cases} \tag{4}$$

Figure 1 shows the results of $n(c, t)$ versus c for different time stages. The curves were plotted based on the calculations of Eq. (1) and on the conditions given by Eqs (3) and (4). The results reveal that there is a saturation tendency in the evolution process of collective short cracks (dashed curve). The saturation curve presents the stable distribution of crack density. As the fatigue process progresses, the distribution of crack density gradually tends to the saturation curve from a small to a large value of crack size.

It is assumed that the upper boundary of the saturation area c^* is the maximum crack length $c_{max}(t)$. This assumption implies that only the crack density in the region of $c < c^*$ exhibits a saturation distribution. The fulfilment of the criterion $c^* = c_{max} = c_{cr}$ is equivalent to the statement that a crack with an initial length of zero develops to a crack of critical length c_{cr}. The evolution

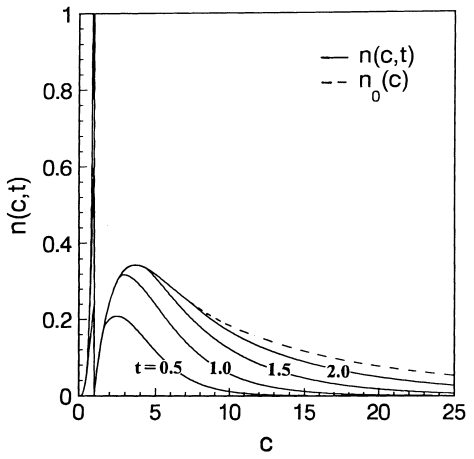

Fig. 1. Variation of crack density $n(c, t)$ with crack length c for different time stages, the dashed curve representing the saturation distribution. The curves were calculated under the conditions of $A_d = 0$, and $\bar{d} = 1$ [refer to Eq. (3)]. The non-dimensional time $t = t' \cdot A^*/d'$, with t', d' and A^* being the real time (fatigue cycles), the real grain diameter and the characteristic crack growth rate, respectively. For example, when $d' = 50$ μm and $A^* = 10^{-3}$ μm/cycle, then $t' = 5 \times 10^4$ for $t = 1$.

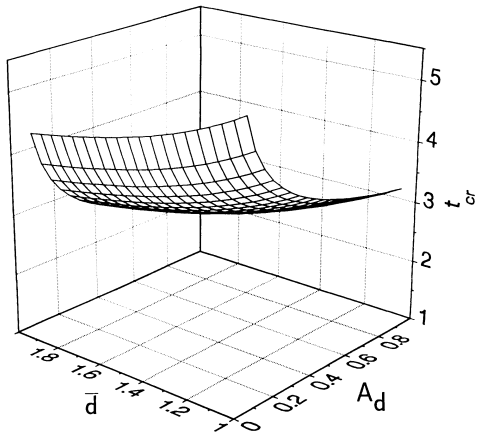

Fig. 2. The critical time t_{cr} as a function of parameters A_d and $\bar{d}$ [refer to Eq. (3)].

© 1998 Blackwell Science Ltd

of c_{max} is

$$c_{max} = c^* = \begin{cases} \dfrac{1}{1-A_d}\{1-\exp[-t(1-A_d)]\} & (t \leqslant t_0) \\ \beta_0 \cdot \exp(\bar{d} \cdot t) & (t > t_0) \end{cases} \tag{5}$$

where

$$t_0 = \frac{1}{\bar{d}} \ln \frac{1}{\beta_0} \quad \text{and} \quad \beta_0 = A_d^{\bar{d}/(1-A_d)}.$$

Note that the total number of cracks is

$$D_0 = \int_0^\infty n(c, t)\, dc = \alpha_0 \cdot t \tag{6}$$

with

$$\alpha_0 = \int_0^\infty N_g \cdot n_N(c, t)\, dc \tag{7}$$

Substituting Eq. (6) into Eq. (5), one can show:

$$c_{max} = \begin{cases} \dfrac{1}{1-A_d}\left[1-\exp\left(-\dfrac{1-A_d}{\alpha_0} \cdot D_0\right)\right] & (t \leqslant t_0) \\ \beta_0 \cdot \exp\left(\dfrac{\bar{d} \cdot D_0}{\alpha_0}\right) & (t > t_0) \end{cases} \tag{8}$$

Equation (8) illustrates the variation of c_{max} with A_d and $\bar{d}$. It is obvious that c_{cr} is greater than 1. Hence, the critical time t_{cr} for the termination of the short-crack regime can be derived from Eq. (5):

$$t_{cr} = t|_{c_{max}=c_{cr}} = \frac{1}{\bar{d}} \ln \frac{c_{cr}}{\beta_0} \tag{9}$$

Figure 2 shows the relationship between t_{cr} and the parameters of A_d and $\bar{d}$ based on Eq. (9). It is seen that the value of t_{cr} increases with a decrease in the values of A_d and $\bar{d}$, suggesting that the tolerance of collective short-crack damage is enhanced if the material is of small grain size and there is a large obstacle effect of the grain boundary against crack growth.

Apparently, Eq. (9) shows that t_{cr} is linearly proportional to $1/\bar{d}$. Considering that short-crack regime covers a large portion of fatigue life, we estimate that fatigue life is also proportional to $1/\bar{d}$. Replacing $\bar{d}$ by d_0, we may write

$$N_f = b_1 + b_2 \frac{1}{d_0} \tag{10}$$

where b_1 and b_2 are parameters related to applied fatigue loading excursions.

DIMENSIONAL ANALYSIS OF FATIGUE DAMAGE EVOLUTION

We define a parameter $P(c)$ which is a function of the energy dispersion due to the development of cracks with length c. In the short-crack regime, the energy dispersion is dominated by the crack

 © 1998 Blackwell Science Ltd

growth process [17], and the variables (d and A_d) that affect crack growth rate are taken into account in the analysis. In addition, $P(c)$ is correlated with the effective stress level, which is a function of the number of cracks [17]. Therefore, we may write,

$$P^{(0)} = P^{(0)}(c, d, A_d, \sigma) \tag{11}$$

where $P^{(0)}$ is a continuous function, and the superscript '(0)' denotes that the validity of the equation is within the short-crack regime. The previous result shows that the crack growth rate is dependent on d and A_d. Hence, using the Π-theorem [18], one may write the non-dimensional form of Eq. (11) as

$$\frac{P^{(0)}}{\sigma \cdot d \cdot A_d} = g\left(\frac{c}{d}\right) \tag{12}$$

For the case of fatigue damage by long cracks, the total energy release rate (Q) caused by the development of the damage system is predominately produced by long cracks, where the effective stress is less sensitive to the damage progression [17]. Thus, Q is adopted to describe the damage extent, i.e.

$$P^{(1)} = P^{(1)}(c, M, Q) \tag{13}$$

where the superscript '(1)' denotes that the validity of the equation is within the long-crack regime. Again, using the Π-theorem [18], one may write the non-dimensional form of Eq. (13) as

$$P^{(1)} = \frac{f_2 \cdot Q}{c} \tag{14}$$

For the total fatigue damage, $P(c)$ is composed of $P^{(0)}$ and $P^{(1)}$, and is derived by $c \to 0$ for the short-crack regime and $c \to c_1$ for the long-crack regime:

$$P(c) = \left(1 - \frac{c}{c_1}\right) P^{(0)}|_{c\to 0} + \frac{c}{c_1} P^{(1)}|_{c\to c_1} = \left(1 - \frac{c}{c_1}\right) f_1 \sigma A_d d + \frac{c}{c_1^2} f_2 Q \tag{15}$$

where $f_1 = g(0)$. It is easy to see the two extremes, i.e. where $P(c)$ tends to $P^{(1)}$ at $c = c_1$, and tends to $P^{(0)}$ at $c = 0$. Referring to the definition of Q and Eq. (15), we have

$$Q = \int_0^{c_1} P(c)\, \mathrm{d}c = f_1^* \sigma A_d dc_1 + f_2^* Q \tag{16}$$

or

$$Q = \frac{f_1^* \sigma A_d dc_1}{1 - f_2^*} \tag{17}$$

in which, $f_1^* = f_1/2$ and $f_2^* = f_2/2$.

Invoking the relationship between the variables of the damage process proposed by Kachanov [19], one may show

$$\sigma = \frac{\sigma_0}{1 - D} \tag{18}$$

We also assume that

$$c_1 = a \cdot D^b \tag{19}$$

© 1998 Blackwell Science Ltd

where a and b are material constants. Substitution of Eqs (18) and (19) into (17) gives

$$Q(D) = \frac{\xi \cdot D^b}{1 - D} \tag{20}$$

with $\xi = af_1^* A_d d\sigma_0/(1 - f_2^*)$.

On the other hand, the parameter of the damage moment which is a product of crack density and crack length, can be used for the description of fatigue damage [17]. A series of damage moments is generally defined as

$$D_m = \gamma \int_0^\infty n(c, t) \cdot c^m \, \mathrm{d}c \tag{21}$$

where $m = 0, 1, 2, \ldots$. The first order of damage moment which represents the total crack length, is

$$D_1 = \gamma \int_0^\infty n(c, t) \cdot c \, \mathrm{d}c \tag{22}$$

Comparing with Eq. (20), one may write

$$Q(D_1) = \frac{\xi \cdot D_1^b}{1 - D_1} \tag{23}$$

It is reasonable to consider that the evolution rate of D_1 is linearly related to $Q(D_1)$, which may be regarded as the damage evolution in the material according to Maugin *et al.*'s theory [20], and that the damage accumulation is mainly produced by crack growth rather than crack nucleation. Hence,

$$\dot{D}_1 = \frac{1}{G}[Q(D_1)] = \frac{\xi^* \cdot D_1^b}{1 - D_1} \tag{24}$$

with $\xi^* = \xi/G$. The development of D_1 from 0 to 1 corresponds to the whole fatigue damage process. Therefore, the fatigue life can be derived as

$$N_f = \int_0^1 \frac{1}{\dot{D}_1} \mathrm{d}D_1 = \int_0^1 \frac{1 - D_1}{\xi^* \cdot D_1^b} \mathrm{d}D_1 = \frac{\kappa}{d \cdot A_d \cdot \sigma_0} \tag{25}$$

where $\kappa = G(1 - f_2^*)/[a \cdot f_1^*(b - 2)(b - 1)]$. Equation (25) indicates that N_f is inversely proportional to the grain size d, which is consistent with the previous derivation of Eq. (10).

EXPERIMENTS AND RESULTS

The material used in this study is a stainless steel with the chemical composition (wt%) of C = 0.098, Si = 0.57, Mn = 1.47, P = 0.027, S = 0.007, Cr = 17.7, Ni = 9.38. Four groups of specimens were prepared using different procedures of heat treatment, in order to produce four groups (A, B, C, D) of different average grain sizes: A = 50 μm, B = 72 μm, C = 130 μm and D = 207 μm. Fatigue testing was performed in an MTS machine at room temperature and the type of specimen is shown in Fig. 3. The stress ratio $R = 0.1$ and frequency $f = 35$ Hz were applied throughout the fatigue tests. For each group of specimens, the number of loading cycles to fracture at a given maximum stress level was recorded. The threshold stress σ_* is defined as the maximum stress ($R = 0.1$) experienced by a specimen withstanding 5×10^6 loading cycles. Figure 4 shows the results of

 © 1998 Blackwell Science Ltd

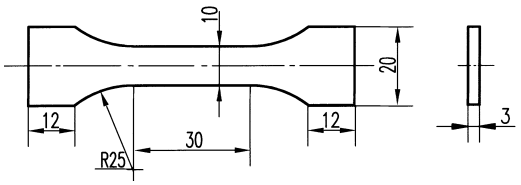

Fig. 3. Geometry of specimen used in fatigue testing, dimensions in mm.

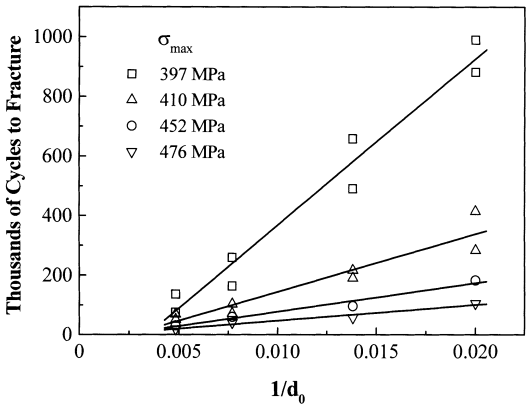

Fig. 4. Fatigue life versus $1/d_0$ for four stress levels, dimension of d_0 in μm.

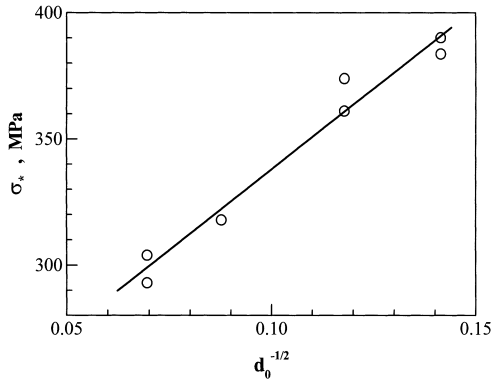

Fig. 5. The fatigue crack growth threshold stress, σ_* versus $d_0^{-1/2}$ for four groups of specimens, dimension of d_0 in μm.

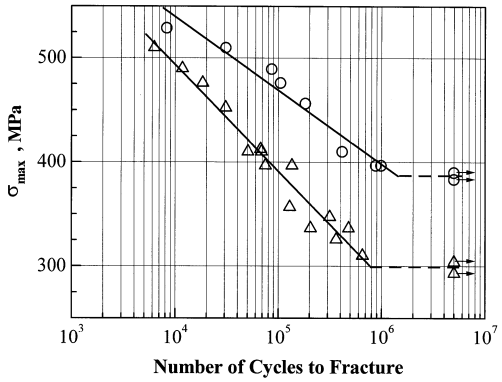

Fig. 6. Maximum applied stress σ_{max} versus number of cycles to failure for Group A specimens (○: $d_0 = 50$ μm) and Group D specimens (△: $d_0 = 207$ μm). The solid curves showing the relation of Eq. (31) and symbols with an arrow indicating that no fracture occurred.

N_f versus $1/d_0$ at four maximum stress levels, and Fig. 5 shows the results of σ_* as a function of grain size for the four groups of specimens. Figure 6 shows the results of the entire S–N data for the two groups of specimens, one with the smallest grain size (Group A, $d_0 = 50$ μm) and one with the largest grain size (Group D, $d_0 = 207$ μm). The data of Group B ($d_0 = 72$ μm) and Group C ($d_0 = 130$ μm) are distributed within the datum band bounded by Group A and Group D, with Group B being superior to Group C.

From Fig. 4, it is seen that the difference in N_f at the given range of stress levels (397–476 MPa) becomes increasingly large as the grain size tends to the small side, and that at the same maximum stress level, N_f is linearly proportional to $1/d_0$. This result is in good agreement with Eqs (10) and (25). Using the method of linear regression, we obtain:

$$N_f = -189 \times 10^3 + 55.7 \times 10^6 \frac{1}{d_0} \tag{26}$$

© 1998 Blackwell Science Ltd

with $r = 0.98$, for $\sigma = 397$ MPa;

$$N_f = -49.6 \times 10^3 + 19.4 \times 10^6 \frac{1}{d_0} \tag{27}$$

with $r = 0.95$, for $\sigma = 410$ MPa;

$$N_f = -19.1 \times 10^3 + 9.63 \times 10^6 \frac{1}{d_0} \tag{28}$$

with $r = 0.98$, for $\sigma = 452$ MPa; and

$$N_f = -6.44 \times 10^3 + 5.33 \times 10^6 \frac{1}{d_0} \tag{29}$$

with $r = 0.98$, for $\sigma = 476$ MPa.

From Fig. 5, we see that σ_* is linearly proportional to $d_0^{-1/2}$, and the following expression is obtained by linear regression:

$$\sigma_* = \alpha + \beta \cdot d_0^{-1/2} \tag{30}$$

with $\alpha = 210$ (MPa), $\beta = 1275$ (MPa $\cdot$ $\mu m^{1/2}$) and the linear correlation coefficient r = 0.984.

From Fig. 6, it is seen that the distribution of N_f against σ_{max} exhibits a linear tendency in a semilogarithmic scale:

$$1g\ N_f = \alpha_1 + \beta_1 \sigma_{max} \tag{31}$$

After the linear regression, we obtain $\alpha_1 = 11.3$, $\beta_1 = -0.0135$ and $r = -0.975$ for Group A (397 MPa $< \sigma_{max} <$ 529 MPa); and $\alpha_1 = 8.65$, $\beta_1 = -0.00934$ and $r = -0.980$ for Group D (310 MPa $< \sigma_{max} <$ 510 MPa). Comparing Eq. (31) with Eq. (25), and converting common logarithm to natural logarithm, one finds that

$$\kappa^* = a' d_0 \sigma_{max} \exp(b' \sigma_{max}) \tag{32}$$

where a' and b' are parameters related to the fatigue resistance of the material.

CONCLUSIONS

Methods based on the equilibrium of crack density and a dimensional analysis were used to study the short-fatigue-crack evolution and to evaluate the fatigue life as influenced by grain size. The fatigue testing of four groups of specimens of a stainless steel, with grain sizes ranging from 50 μm to 207 μm, was performed to reveal the effect of grain size on fatigue resistance. The following conclusions are drawn:

(1) The critical time t_{cr} characterizing the termination of the short-crack regime is influenced by the normalized grain size $\bar{d}$ and the obstacle effect of the grain boundary A_d. The value of t_{cr} becomes larger with a decrease in $\bar{d}$ and increases with a reduction in A_d.
(2) The formulae derived by theoretical analyses show that the fatigue life is inversely proportional to grain size.
(3) Experimental results show a linear relationship between N_f and d_0^{-1} for a given maximum stress level, which is in good agreement with the theoretical analyses.
(4) Experimental results show a linear correlation between σ_* and $d_0^{-1/2}$, and a linear correlation between lg N_f and σ_{max}.

 © 1998 Blackwell Science Ltd

Acknowledgements—This paper was supported by the National Outstanding Youth Scientific Award of China, the National Natural Science Foundation of China, and the Chinese Academy of Sciences.

REFERENCES

1. J. Lankford (1982) The growth of small fatigue cracks in 7076-T6 aluminum. *Fatigue Engng Mater. Struct.* **5,** 233–248.
2. A. K. Zurek, M. R. James and M. L. Morris (1983) The effect of grain size on fatigue crack growth of short cracks. *Metall. Trans.* **14A,** 1697–1705.
3. A. Fathulla, B. Weiss and R. Stickler (1986) Short fatigue cracks in technical Pm-Mo alloys. In: *The Behaviour of Short Fatigue Cracks* (Edited by K. J. Miller and E. R. de los Rios), Mechanical Engng Publisher, London, pp. 115–132.
4. A. Navarro and E. R. de los Rios (1987) A model for short fatigue crack propagation with an interpretation of the short-long crack transition. *Fatigue Engng Mater. Struct.* **10,** 169–186.
5. M. Goto (1994) Statistical investigation of the behaviour of small cracks and fatigue life in carbon steels with different ferrite grain sizes. *Fatigue Fract. Engng Mater. Struct.* **17,** 635–649.
6. J. Weiss and A. Pineau (1993) Continuous and sequential multiaxial low-cycle fatigue damage in 316 stainless steel. In: *Advance in Multiaxial Fatigue* (Edited by D. L. McDowell and R. Ellis), ASTM STP 1191, American Society for Testing and Materials, Philadelphia, pp. 183–203.
7. Y. Hong, Z. Gu, B. Fang and Y. Bai (1997) Collective evolution characteristics and computer simulation of short fatigue cracks. *Phil. Mag. A.* **75,** 1517–1531.
8. Y. Hong, Y. Lu and Z. Zheng (1989) Initiation and propagation of short fatigue cracks in a weld metal. *Fatigue Fract. Engng Mater. Struct.* **12,** 323–331.
9. Y. Hong, Y. Lu and Z. Zheng (1991) Orientation preference and fractal character of short fatigue cracks in a weld metal. *J. Mater. Sci.* **26,** 1821–1826.
10. C. M. Suh, J. J. Lee, Y. G. Kang, H. J. Ahn and B. C. Woo (1992) A simulation of the fatigue crack process in type 304 stainless steel at 538 °C. *Fatigue Fract. Engng Mater. Struct.* **15,** 671–684.
11. A. Turnbull and E. R. de los Rios (1995) The effect of grain size on fatigue crack growth in an aluminium magnesium alloy. *Fatigue Fract. Engng Mater. Struct.* **18,** 1355–1366.
12. M. Kage, K. J. Miller and R. A. Smith (1992) Fatigue crack initiation and propagation in a low-carbon steel of two different grain sizes. *Fatigue Fract. Engng Mater. Struct.* **15,** 763–774.
13. G. T. Gray, A. W. Thompson and J. C. Williams (1983) The effect of micro-structure on fatigue crack path and crack growth rate. In: *Fatigue Crack Growth Threshold Concepts* (Edited by D. Davidson and S. Suresh), AIME, New York, pp. 131–145.
14. B. Fang, Y. Hong and Y. Bai (1995) Experimental and theoretical study on numerical density evolution of short fatigue cracks. *ACTA Mechanica Sinica* (*English Edition*) **11,** 144–152.
15. F. Ke, Y. Bai and M. Xia (1990) Evolution of ideal micro-crack system. *Science in China A* **6,** 621–631 (in Chinese).
16. J. M. Kendall and J. E. King (1988) Short fatigue crack growth behaviour: data analysis effects. *Int. J. Fracture* **10,** 163–170.
17. Y. Hong and Y. Qiao (1997) Analysis of damage moments in the collective evolution of short fatigue cracks. *Key Engng Mater.* **145–149,** 399–404.
18. F. W. David and H. Nolle (1982) *Experimental Modeling in Engineering*, Butterworth, New York.
19. L. M. Kachanov (1986) *Introduction to Continuum Damage Mechanics*, Martinus Nijhoff, The Netherlands.
20. G. A. Maugin, E. Marcelo and C. Trimarco (1992) Pseudo-momentum and material force in damage of metals. *Int. J. Solids Structures.* **29,** 1889–1900.

© 1998 Blackwell Science Ltd